Current Research in Biotechnology 4 (2022) 428–439

Contents lists available at ScienceDirect

Current Research in Biotechnology

journal homepage: www.elsevier.com/locate/crbiot

# Manipulation of viral protein production using the PCNA of halovirus ϕCh1 via alternative start codon usage

Richard John Manning [a], Michael Tschurtschenthaler [b], Sonja Sabitzer [c], Angela Witte [a,*]

[a] Department of Microbiology, Immunobiology and Genetics, Max Perutz Labs, University of Vienna, Vienna, Austria
[b] VelaLabs GmbH, Brunner Str. 69/3, 1230 Vienna, Austria
[c] VetCORE - Facility for Research, Vetmeduni Vienna, Vienna, Austria

## ARTICLE INFO

*Keywords:*
PCNA
*Natrialba magadii*
ϕCh1, Halovirus

## ABSTRACT

Proliferating Cell Nuclear Antigen (PCNA) is a scaffold protein principally found at the centre of replication, coordinating with a wide array of interaction partners. ϕCh1, unusually for a virus, encodes a putative PCNA. *Natrialba magadii,* the only known host of ϕCh1, also encodes a putative PCNA of high sequence similarity, differing in the presence of an alternate GUG start codon 5′ of the AUG start codon resulting in a larger protein. Homologous recombination was used to delete the viral PCNA gene. Complementation and overexpression strains with plasmid expressed viral PCNA variants were created and analyzed for growth and lytic behaviour, viral protein levels, and virus titer. Deletion of ϕCh1 ORF59, encoding $PCNA_{\phi Ch1}$ resulted in a significant reduction in the virus titer, reduced viral protein load, and reduced lysis. Complementation and overexpression with WT and mutant variants of ORF59 revealed that modification of the GTG start codon to ATG changes the life cycle in terms of production of progeny virus particles. The different variants have a broad range of variable effects on each of the phenotypes observed. Experiments with a halophilic beta-galactosidase assay revealed a *cis/trans* mediated interaction between the viral PCNA and the origin of replication of ϕCh1 modulated by the 5′GTG to ATG sequence. The virally encoded PCNA is not essential, but is crucial, to the life cycle of the virus ϕCh1. The 5′ region upstream of the primary AUG codon and its regulation with an alternate start codon is essential to the homeostasis of the virus-host relationship.

**Contents**



* Corresponding author.
*E-mail address:* angela.witte@univie.ac.at (A. Witte).

https://doi.org/10.1016/j.crbiot.2022.09.006
Received 31 May 2022; Revised 8 September 2022; Accepted 13 September 2022

ϕCh1 is a model for haloalkaliphilic viruses and infects the haloalkaliphilic archaeon *Natrialba magadii* (Tindall et al., 1984). As typical for members of the *Myoviridae* family, ϕCh1 consists of an icosahedral head and a contractible tail and contains a dsDNA genome (Witte et al., 1997). The halovirus ϕCh1 is adapted to the extreme growth conditions of its host *N. magadii*, depending on high salt concentrations (4–5 M NaCl) and high pH values (8.5–11) (Witte et al., 1997). ϕCh1 was originally identified as prophage integrated in the chromosome of the wild-type strain *N. magadii* L11. Induction of the lytic cycle occurs spontaneously in the mid to late logarithmic phase upon which virus particles are produced and released by cell lysis. The cured strain *N. magadii* L13 can be re-infected by ϕCh1 (Witte et al., 1997). The genome of ϕCh1 is completely sequenced; it contains 58.5 kbp and consists of 98 open reading frames (ORFs) (Klein et al., 2002). A set of structural genes is organized in a gene cluster at the 5′ end of the viral genome. Several genes within this cluster show sequence homologies to other halovirus and bacteriophage genes (Klein et al., 2002), and the functions of 12 ORFs of ϕCh1 have been identified experimentally (Klein et al., 2000). In additions two transcriptional regulators were analyzed in more detail (Iro et al., 2007; Selb et al., 2017).

Proliferating Cell Nuclear Antigen (PCNA) is the "*Maestro of the Replication Fork*", *"a dancer with many partners*" and stands "*on the crossroad of Cancer*". It is a crucial processivity factor and binding scaffold in the replication fork from which point it regulates the activity of a wide array of proteins and plays a key role in cell function and activity including cancer genesis (Moldovan et al, 2007; Maga and Hubscher, 2003; Stoimenov and Helleday, 2009). PCNA forms a trimeric sliding clamp in Eukarya and Archaea, homologous to the dimeric β-clamp of Bacteria (Maga and Hübscher, 2003) The second and third domains of the β-sliding clamp of Bacteria share sequence homologies with the PCNA proteins of Archaea and Eukarya, indicating that these proteins all derive from a protein present in the last universal common ancestor and is an essential component of the replisome (Acharya et al, 2021). PCNA is primarily known as an essential component of the replication fork, but also has roles in DNA repair, DNA methylation, chromatin remodeling, and cell cycle regulation (Pan et al, 2011). All activities described for the PCNA proteins require them to encircle the DNA; no enzymatic function for PCNA off DNA has been reported (Pan et al, 2011).

*Natrialba magadii* is a member of the *Halobacteriaceae* family of the *Euryarchaeota* branch of the archaeal domain which also includes the *Crenarchaeota* and *Thaumarchaeota* branches (Pan, Kelman and Kelman, 2011). Most members of the *Euryarchaeota* and *Thaumarchaeota* encode for a single PCNA gene that forms homotrimers, however some members of the crenarchaeota branch contain three distinct PCNA genes that yields an active heterotrimeric form (Ladner et al., 2011; Dionne et al., 2003). The crystal structure of the PCNA of *Haloferax volcanii* (HvPCNA), another member of the *Halobacteriaceae* family, was solved revealing that in comparison to PCNA found in other organisms the positive surface charge at the interior surface of the PCNA trimer was significantly reduced. It is hypothesized that bound cations within the shell of HvPCNA may reduce the effect of electrostatic repulsion and allow sliding along the negatively charged DNA (Winter et al, 2009). HFTV1 an archaeal virus isolated on a *Haloferax* strain was found to also encode for a PCNA with its closest homologs being the PCNA of cellular organisms indicating acquisition from halophilic Archaea (Mizuno et al, 2019).

Unusually for a virus, ORF59 of ϕCh1 encodes a putative PCNA, with a high sequence similarity to a putative PCNA produced by the host indicating recent horizontal gene transfer (Lynch et al., 2012). Processivity factors are found in less than 20 percent of dsDNA virus genomes, of which only a handful are known in Archaea, this makes the putative PCNA of ϕCh1 an intriguing target for analysis (Kazlauskas et al, 2016). Intriguingly, ϕCh1 also encodes an alternate GUG start codon 63 bp upstream of the primary AUG start codon. In the closely related *Haloferax volcanii* only 6% of leaderless transcripts, which constitute the majority of *H. volcanii* transcripts, used the alternate GUG start codon (Babski et al, 2016). The rarity of GUG start codon usage in halophilic Archaea and its potential use by ϕCh1 for an N-terminal extension of the gene encoded by ORF59 relative to the host encoded homolog engendered it as an additional investigative target.

Homologous recombination was used to disrupt ORF59 of ϕCh1. Complementation and overexpression strains containing ORF59 plasmid expressed variants were analysed for lytic behaviour, viral protein levels with Western blots, and virus titers. In addition, reporter gene assays were used to investigate the interactions between to origin of replication of ϕCh1 and the different variants of ORF59. These experiments were undertaken to determine the function of ORF59 and the 63 bp region encoded under the translational control of the GUG start codon.

## 2. Materials and methods

All PCRs for the amplification of DNA for the purposes of cloning were performed using Phusion High-Fidelity DNA Polymerase according to the manufacturer's instructions (Thermo Fisher Scientific Inc., Waltham, MA, USA). PCRs for screening of *N. magadii* and *E. coli* transformants were performed using GoTaq® DNA Polymerase according the to manufacturer's instructions (Promega Corporation, Madison, WI, USA). All strains, plasmids and primers used in this study are listed in Appendix A.

ORF59 of ϕCh1 was amplified using primers p30-5/p30-3 (744 bp) and ϕCh1 DNA as a template, the amplified fragment was restricted with *Bgl*II and *Hind*III and ligated into pRSET-A also restricted with the *Bgl*II and *Hind*III, resulting in plasmid pPol5 which was transformed into *E. coli* Bl21(DE3) competent cells. ORF59 was expressed and the PCNA protein was purified using the same method as previously reported (Selb et al., 2017). Protein was isolated twice and used for the generation of two separate rabbit polyclonal antibody sera (α-PCNA_1 and α-PCNA_2) (Moravian-Biotechnology, Ltd., Brno, Czech Republic).

ORF59 of ϕCh1 was deleted using the homologous recombination plasmid pKSII-PCNA1-5-NovR-R created as follows. The region upstream of ORF59 was amplified using ϕCh1 DNA as template with the primers ΔPCNA-1/ΔPCNA-2 (1240 bp), the fragment and pKSII + were separately restricted with *Xba*I and *Sma*I, purified, and ligated together. Positive clones were named pKSII-PCNA1-2. The flanking region downstream of ORF59 was PCR amplified with ΔPCNA-3 /ΔPCNA-5 (629 bp), restricted with *Hind*III and *Kpn*I and ligated into pKSII-PCNA1-2 also digested with *Hind*III and *Kpn*I. Positive clones were named pKSII-PCNA-1–5. The *gyr*B gene was released from pMDS11 (Holmes et al, 1991) with *Hind*III and *Sma*I (2448 bp) and ligated into plasmid pQE30 restricted with *Hind*III and *Sma*I resulting in plasmid pQE-30-NovR. The *gyr*B was amplified from pQE-30-NovR with primers NovR-1p/NovR-1 s (2453 bp), restricted with *Pst*I and *Sma*I and ligated into pUC19 also restricted with *Pst*I and *Sma*I resulting in pUC19-NovR" reverse". The *gyr*B gene (2453 bp) was released from the vector pUC19-NovR "reverse" with *Sma*I, and *Pst*I, and ligated into pKSII-PCNA-1-5 digested with *Sma*I and *Pst*I, creating pKSII-PCNA-1-5-novR "reverse"(pKSII-PCNA1-5-NovR-R).

*N. magadii* L11 contains the provirus ϕCh1 and *N. magadii* L13, the cured strain, lost the virus and was used for virus titer analysis (Witte et al., 1997).

**Table 1**
Strains created for the analysis of $PCNA_{\Phi Ch1}$. Features: [1]: wild type PCNA starting with codon GTG, [2]: changed GTG codon to ATG, [3]: truncated version starting with ATG, same size as the host encoded PCNA. $N_{60}$ represents the 60 nucleotides between the GTG and the ATG.

| Strains | | |
|---|---|---|
| **Overexpression** | **Complementation** | **Feature** |
| *N. magadii* L11 (pNB102) | *N. magadii* L11-ΔPCNA (pNB102) | Control |
| *N. magadii* L11 (pPCNA-GTG) | *N. magadii* L11-ΔPCNA (pPCNA-GTG) | GTG-$N_{60}$-ATG[1] |
| *N. magadii* L11 (pPCNA-ATG) | *N. magadii* L11-ΔPCNA (pPCNA-ATG) | ATG-$N_{60}$-ATG[2] |
| *N. magadii* L11 (pPCNA-Tr) | *N. magadii* L11-ΔPCNA (pPCNA-Tr) | ATG[3] |

pKSII-PCNA1-5-NovR-R was transformed into competent *N. magadii* L11 as previously reported (Selb et al., 2017). Resultant colonies were PCR tested for the presence of 5′ homologous crossover with primers 56–5/Nov-13 (1992 bp) and 3′ crossover with Nov-12/PCNA-3en (1065 bp). A homozygous mutant strain was obtained using the same method as previously reported for ORF79 of ϕCh1 (Selb et al, 2017). Following homozygation of the mutant, individual colonies were again tested for the presence of both 3′ and 5′ crossover as well as for the absence or presence of the ORF59 with p30-5/p30-3(764 bp). The results of the PCR data were confirmed by Southern blot genotyping was carried as previously reported (Selb et al, 2017) and the positive strain designated as *N. magadii* L11-ΔPCNA (Fig. A1).

The promotor region of ORF34 of ϕCh1 was amplified from ϕCh1 template DNA with 34-p5-Xba1/34-p3 (326 bp), restricted with *BamH*1 and *Xba*I and ligated into pKSII + also restricted with *BamH*1 and *Xba*I resulting in plasmid pKS-34up.

The variants of ORF59 were amplified with PCNA-GTG/PCNA-22 (827 bp), PCNA-ATG/PCNA-22 (827 bp), and PCNA-Tr/PCNA-22 (754 bp), restricted with *EcoR*I and *Kpn*I. Fragments were ligated into pKS-34up restricted with *EcoR*I and *Kpn*I resulting in plasmids pKS-34up-P-GTG, pKS-34up-P-ATG, pKS-34up-P-Tr. The promotor region of ORF34 and ORF59 were released from the plasmids with *Xba*I and *Kpn*I and ligated in pNB102 likewise restricted with *Xba*I and *Kpn*I. Resulting in the construction of three complementation plasmids pPCNA-GTG, pPCNA-ATG, and pPCNA-Tr respectively.

Each of the complementation plasmids and pNB102 were transformed into *N. magadii* L13. Each of the four resultant strains was then infected with virus particles from either *N. magadii* L11 or *N. magadii* L11-ΔPCNA using a reinfection strategy as previously reported (Selb et al, 2017) resulting in 8 strains for analysis (see Table 1).

Strain L13 of *N. magadii* was transformed with the shuttle vector pRo-5/BgaH containing the haloarchaeal betagalactosidase gene *bga*H under the control of the ORF48-49 intergenic promotor region of ϕCh1.

ORF59 gene variants were amplified from pPCNA-ATG, pPCNA-Tr, and pPCNA-GTG using primers IR-PCNA-1_1/ IR-PCNA-2_1 (1203 bp, 1130 bp, 1203 bp) and ligated into pRo-5/BgaH restricted with *Not*I. Resulting in plasmids pMI-PCNA-ATG, pMI-PCNA-Tr and pMI-PCNA-GTG.

The resultant strain *N. magadii* L13 (pRo-5/BgaH) was transformed with the pNB102 shuttle vectors containing the ϕCh1 PCNA variants and an empty pNB102 shuttle vector resulting in the strains *N. magadii* L13 (pRo-5/BgaH, pNB102), *N. magadii* L13 (pRo-5/BgaH, pPCNA-ATG), *N. magadii* L13 (pRo-5/BgaH, pPCNA-Tr), and *N. magadii* L13 (pRo-5/BgaH, pPCNA-GTG). Each of the PCNA containing strains was isolated in triplicate and in duplicate for the empty pNB102 containing strain.

The 5′ and 3′ fragments of the GTG and ATG variants of ORF59 were amplified from pPCNA-ATG and pPCNA-GTG using primers IR-PCNA-1_1/ PCNA-ΔATG-2 (416 bp) and IR-PCNA-1_1/ IR-PCNA-2_1 (768 bp), these fragments were assembled along with pRo-5/BgaH restricted with *Not*I via Gibson assembly (Gibson et al., 2009) resulting in plasmids pMI-PCNA-ATG-ΔATG and pMI-PCNA-GTG-ΔATG.

All *N. magadii* strains used in this study were grown in rich medium containing 8.8 g $l^{-1}$ of casein hydrolysate and 11.7 g $l^{-1}$ yeast extract in 4 M NaCl, 1 mM $MgSO_4$, 0.02 mM $FeSO_4$, 36 mM $Na_2CO3$, 31.5 mM KCl, and 3 mM $Na_3$-citrate, at 37 °C shaking at 160 rpm. Optical density was measured at 600 nm. Novobiocin and mevinolin were added to a final concentration of 3 and 7.5 μg/ml, respectively.

Spheroblast generation, transformation, and transformant screening in *N. magadii* strains was performed as previously reported (Mayrhofer-Iro et al., 2013): Fresh pre-culture of the strain to be transformed was inoculated NVM (60 ml) with bacitracin (70 μg/ml) to an $OD_{600}$ of 0.1 and incubated for a maximum of 24 h or until the culture reached on $OD_{600}$ of 0.5–0.6. The culture was centrifuged at 5500g for 15 min at room temperature. The supernatant was discarded and the pellet resuspended in 30 ml of buffered high salt spheroblasting solution and proteinase K (0.1%) and incubated at 42 °C shaking until the majority of the cells were spherical.

For each transformation 1.5 ml of the spheroblasts was used. The cells were pelleted by centrifugation at 10 000g for 15 min at room temperature and resuspended in 150 μl of buffered high salt spheroblast solution. 15 μl of 0.5 M EDTA was added to the cells and incubated for 10 min at room temperature. DNA for transformation was added to the cells in a maximum volume of 10 μl of $H_2O$. For shuttle vector transformations 3-5μg of plasmid DNA was used. For suicide plasmids for the purposes of homologous recombination a minimum of 30μg of DNA was used. The cells plus DNA were incubated at room temperature for 5 min. 150 μl of 60% PEG-600 in unbuffered high salt spheroblasting solution was added and incubated at room temperature for 30 min. The cells were then washed by the addition on 1 ml of NVM followed by gentle mixing and then centrigation at 10 000g for 5 min at room temperature. The supernatant was discarded and the pellet resuspended in 1 ml of NVM and incubated at 37 °C shaking at 160 rpm. Every 24 h the cells were examined, if the majority of cells were still spheroblasts the cells were washed again in 1 ml of $NVM^+$ and re-incubated. Once the majority of cells had regenerated their rod shaped morphology the cells were plated out. NVM selective media plates were used for plating. The plates were incubated at 42 °C until colonies were visible.

DNA isolation from halophilic *Archaea*. Chromosomal DNA of *N. magadii* was isolated by phenol–chloroform extraction, followed by precipitation with isopropanol as previously described (Witte et al, 1997). Southern blot genotyping was performed as previously described (Klein et al, 2000).

Virus titers were determined as described previously (Witte et al, 1997): 100 μl of serial dilutions were added to 300 μl of *N. magadii* L13 cells and 5 ml of top agar and poured onto an agar plate containing complex medium. The plates were sealed in a plastic bag and incubated for 8 to 9 days at 37 °C.

Cell extracts for Western blot analysis were prepared as described previously (Klein et al, 2000). Western blot analyses were performed as previously described (Harlow and Lane, 1988). Detection was performed with 3 ml of 0.113 mM p-coumaric acid, 1.25 mM 3-Aminophthalhydrazide in $ddH_2O$, and 1 μl of 30% $H_2O_2$ and imaged with Biolabs XRS ChemiDoc.

The samples were analysed for BgaH activity using a protocol from Dyall-Smith (2009) modified for analysis using a 96 well plate reader. Each of the samples was analysed in technical duplicates. To each well was added 20 μl of culture, 20 μl 2% Triton X-100, 120 μl BgaH buffer, and 40 μl of 4 mg/ml ONPG to start the reaction. The plate reader was programmed to shake the samples for 5 min before measuring the absorbance at 405 nm every minute for 20 min. In a separate 96 well plates, the $OD_{600}$ of the cultures was measure by diluting 50 μl of culture with 150 μl of NVM medium.

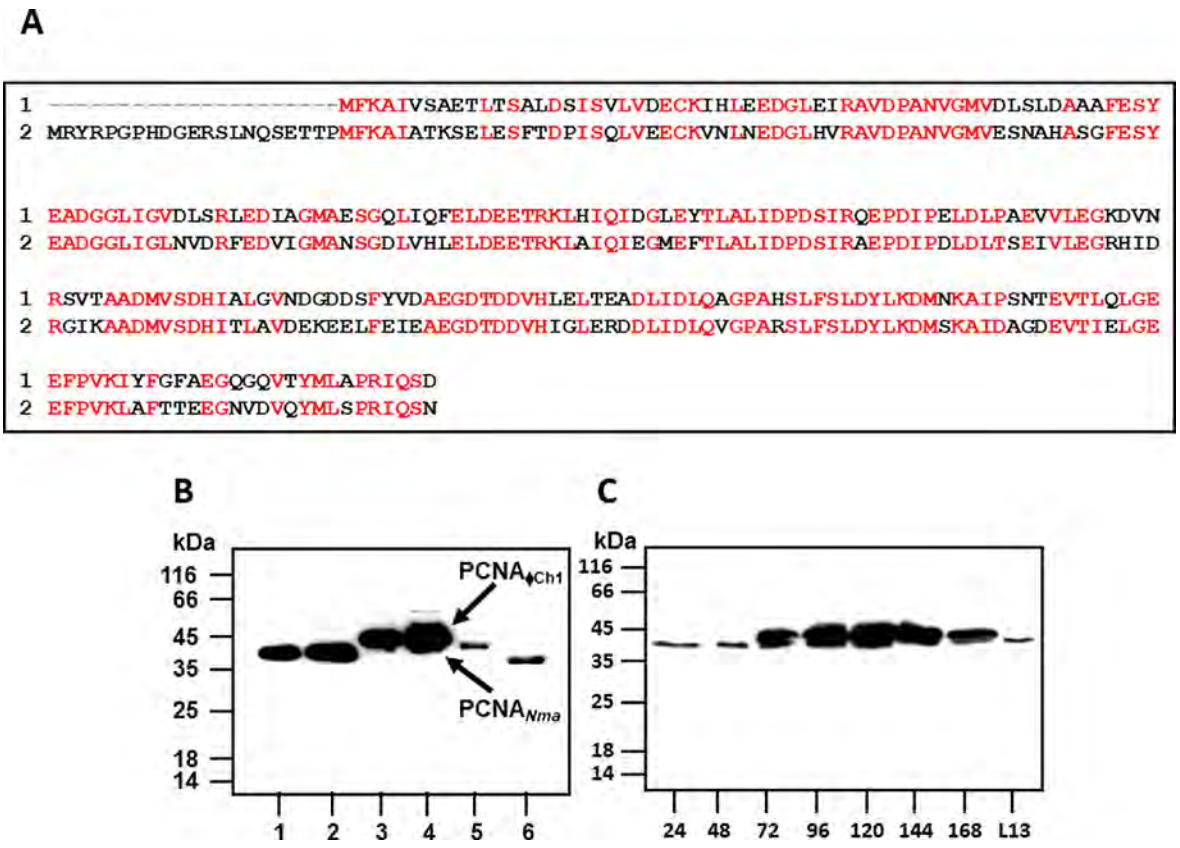


**Fig. 1.** *N. magadii* L11 produces a second larger PCNA protein compared to *N. magadii* L13. (A) Amino acid alignment of 1) $PCNA_{Nab}$ and 2) $PCNA_{\phi Ch1}$ including the N-terminal extension of $PCNA_{\phi Ch1}$. Identical AA are indicated in red. (B) Western blot with α-PCNA_1 of closely related halophilic strains-Lanes: 1) *H. salinarum* $R_1$, 2) *H. salinarum* $R_1$-L, 3) *N. magadii* L11 (72 h), 4) *N. magadii* L11 (120 h) 5) *N. magadii* L13, 6) *H. volcanii*. (C)Western blot analysis of *N. magadii* L11 protein samples taken every 24 h after inoculation with α-PCNA_1, the final lane contains *N. magadii* L13 crude extract as a control. 3 technical replicates were used.

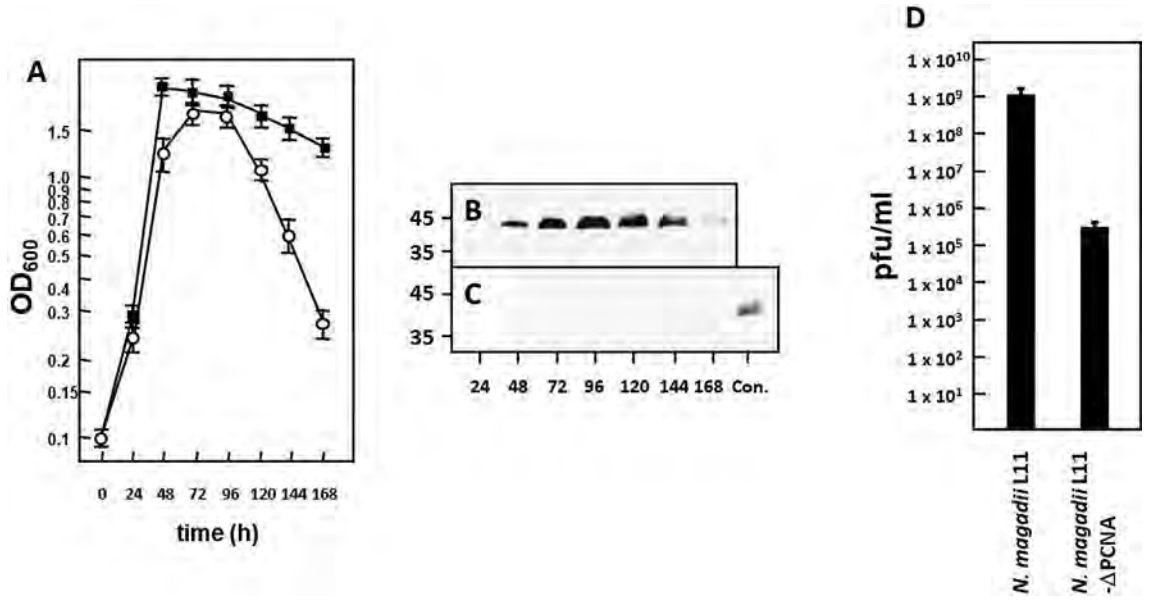


**Fig. 2.** Growth and virus progeny production of the wild type strain *N. magadii* L11 (●) and the mutant strain *N. magadii* L11-ΔPCNA (■). (A) Growth curves of strains *N. magadii* L11 and *N. magadii* L11-ΔPCNA. (B) (C) Western blots of samples taken every 24 h according the growth and lysis curve (A). Western blots were performed with α-PCNA_2. (B) *N. magadii* L11, (C) *N. magadii* L11-ΔPCNA. (C) Con. crude extract of *N. magadii* L11. (D) Virus titers of *N. magadii* L11 and *N. magadii* L11-ΔPCNA at 168 h. 3 biological replicates were used. Error bars are indicated, ±1SD.

To calculate the specific BgaH activity the slope of the increase of absorbance at 405 nm over the observed time period was calculated and used in the following formula SA = (slope*1000)/(0,01*$OD_{600}$).

## 3. Results

### 3.1. Initial analysis

*Natrialba magadii,* the only known host of ϕCh1, also encodes a putative PCNA of high sequence similarity to ORF59 of ϕCh1, differing majorly in the presence of an alternate GUG start codon 5′ of the AUG start codon resulting in a larger protein (Fig. 1A).

A polyclonal antibody with specificity to the ϕCh1 encoded PCNA (α-PCNA_1) was developed. Western blots using this antibody revealed that it's affinity to the PCNAs of *H. volcanii* and *H. salinarum,* and possibly the PCNA produced by the immunity conferring plasmid pϕHL derived from the central L-region of ϕH (Gropp et al., 1992) (Fig. 1B).

Western blots of *N. magadii* L11 crude extracts using this antibody revealed a second higher signal, compared to the cured *N. magadii* L13 strain, appearing 72 h after inoculation with band intensity peaking at 120 h (Fig. 1C). This provides evidence that $PCNA_{\phi Ch1}$ is, at least in part, translated using the alternate GUG start codon encoded upstream of the ATG consensus sequence in ORF59. This raised the question as to whether $PCNA_{\phi Ch1}$ is essential for the replication cycle of ϕCh1.

### 3.2. Construction and analysis of N. magadii L11-ΔPCNA

To determine the relevance of $PCNA_{\phi Ch1}$ a deletion mutant was created using homologous recombination via the suicide plasmid pKSII-PCNA1-5-NovR-R resulting in the deletion of ORF59 and the insertion of the novobiocin resistance conferring gene *gyr*B in the ORF59 locus.

The deletion of ORF59 does not eliminate the lysis phenotype, nor does it affect the timing of lysis induction, however it results in a significant increase in peak $OD_{600}$, and a highly significant increase in post lysis optical density (Fig. 2A). Both *N. magadii* L11 and *N. magadii* L11-ΔPCNA grow similarly for the first 24 h of incubation indicating that the growth of the host during the exponential phase is not affected by $PCNA_{\phi Ch1}$.

The disruption of ORF59 results in a minimum two magnitude decrease in virus titer over all sampled time points, an earlier peak titer compared to wildtype *N. magadii* L11, and an over three magnitude decrease at 168 h (Fig. 2D and Fig. A3). The virus titer data in concert with the growth curve data reveals that $PCNA_{\phi Ch1}$ is not essential for the replication cycle of ϕCh1, but it does play an important role in the ability of the strain to produce viral progeny.

To further investigate the function of $PCNA_{\phi Ch1}$ *N. magadii* L11-ΔPCNA and *N. magadii* L11 were transformed with pNB102 shuttle vectors expressing one of three variants of ORF59 under the control of the promoter region of ORF34 of ϕCh1, which was used as it been previously validated (Selb et al., 2017). Plasmid pPCNA-GTG encodes the "wild-type" of ORF59, pPCNA-ATG has a point mutation of the GTG to ATG compared to pPCNA-GTG, and pPCNA-Tr encodes a 5' truncated variant starting from the ATG sequence comparable to the start codon of the host encoded PCNA gene (Fig. 1A). In addition, both *N. magadii* L11 and *N. magadii* L11-ΔPCNA were transformed with empty pNB102 plasmids, as the presence of the mevinolin selection marker encoded by pNB102 results in a change in growth behavior, possibly due to growth rate limiting effects of the metabolically important mevalonate pathway. A comparison of the growth rates of the strains *N. magadii* L11, *N. magadii* L13, and *N. magadii* L11-ΔPCNA with and without pNB102 can been see in Fig. A2.

### 3.3. Analysis of complementation strains

#### 3.3.1. Growth curves and virus titers of the complemented strains

Complementation of the deletion mutant *N. magadii* L11-ΔPCNA with all three of the ORF59 variants leads to a rescue of the lysis phenotype (Fig. 3A).

Unlike the growth and lysis phenotype, complementation of the deletion strains does not result in a rescue of the virus titer. However,

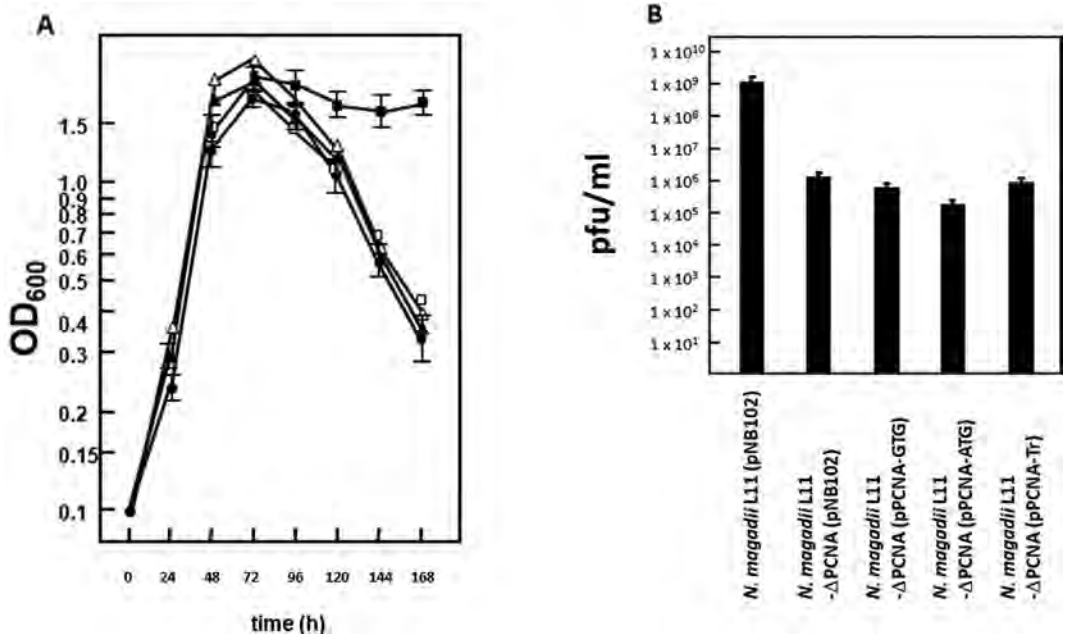


**Fig. 3.** Growth and virus progeny production of the complemented strains (A). Growth curves of the complemented strains *N. magadii* L11-ΔPCNA (pPCNA-GTG) (△), *N. magadii* L11-ΔPCNA (pPCNA-ATG) (▲) and *N. magadii* L11-ΔPCNA (pPCNA-Tr) (❒) with *N. magadii* L11 (pNB102) (●) and *N. magadii* L11-ΔPCNA (pNB102) (■) included as controls. Error bars were shown for strains *N. magadii* L11 (pNB102) (●) and *N. magadii* L11-ΔPCNA (pNB102) (■). (B) Virus titers of samples taken at 168 h from the cultures (A) of the complemented strains with *N. magadii* L11 (pNB102) and *N. magadii* L11-ΔPCNA (pNB102) included as controls. 3 technical replicates were used. Error bars are indicated, ±1SD.

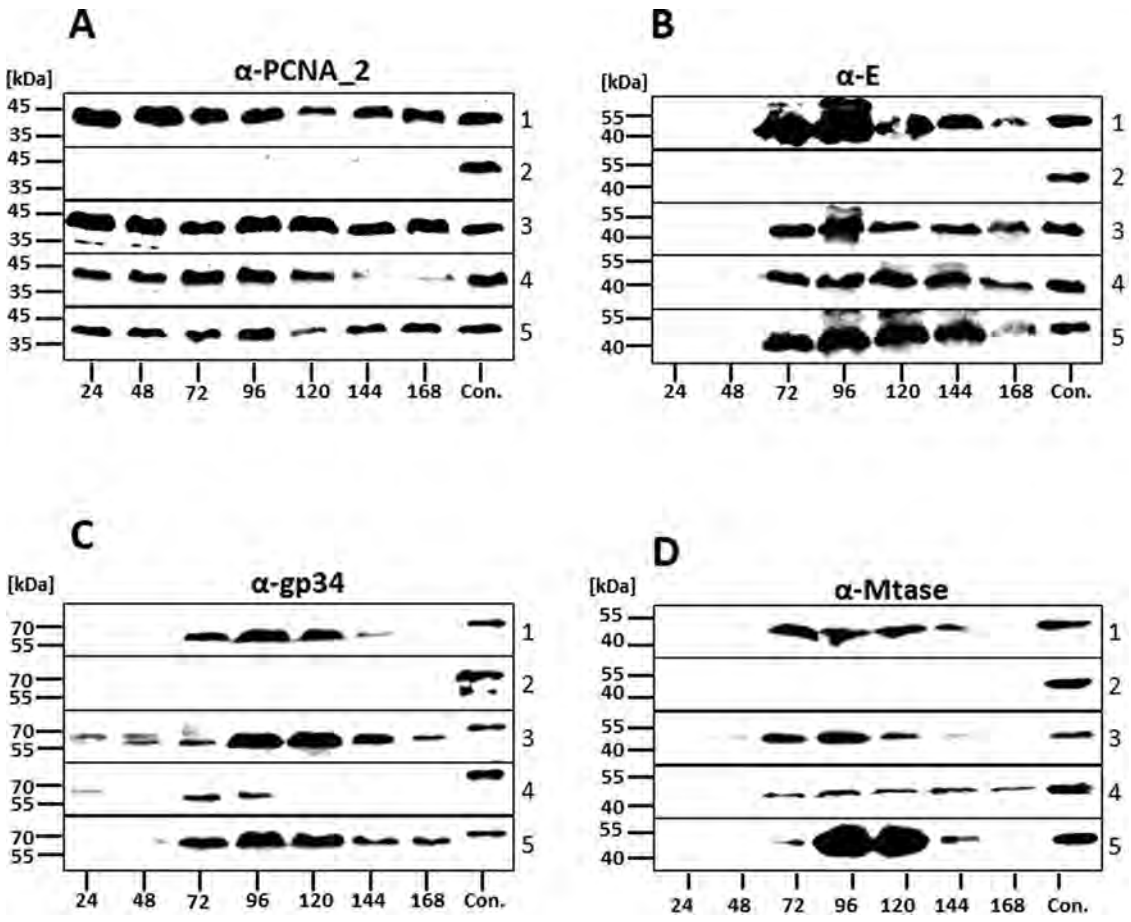


**Fig. 4.** Protein levels of the complemented strains as analysed by Western blot. (A) α-PCNA_2 (B) α-E (C) α-gp34 (D) α-Mtase. 1) *N. magadii* L11 (pNB102), 2) *N. magadii* L11-ΔPCNA (pNB102), 3) *N. magadii* L11-ΔPCNA (pPCNA-ATG), 4) *N. magadii* L11-ΔPCNA (pPCNA-Tr), 5) *N. magadii* L11-ΔPCNA (pPCNA-GTG). Samples were taken 24 to 168 h after inoculation. Con: proteins isolated from *E. coli* were taken as a control in each panel. Size markers are indicated to the left. 3 technical replicates were used.

the virus titer kinetics in the complemented strains in comparison to the un-complemented deletion strain are rescued (Fig. A3). *N. magadii* L11-ΔPCNA (pNB102) has a relatively static virus titer over the analysed time-period, in comparison to the WT strain which has a low virus titer over the first two days, increasing significantly on day three and peaking on day five. The complemented strains, like the WT strain, have a low virus titer on days one and two, with *N. magadii* L11-ΔPCNA (pPCNA-ATG) peaking on day three and the strains complemented with the GTG and truncated variants of ORF59 having a peak virus titer on day four (Fig. A3).

### *3.3.2. Protein production of complemented strains*

In addition, the production of four different proteins were analyzed using western blotting. Here, the virus specific protein PCNA, the methyltransferase (Mtase) M.*Nma*ϕCh1I (Baranyi et al., 2000), the major capsid protein E (Klein et al., 2000) as well as the putative tail fibre gp34 (Rössler et al., 2004; Klein et al., 2012) were used to monitor gene expression within these strains. Proteins E, gp34 and the Mtase were chosen as examples for proteins encoded in the 5´-end, the central region and the 3´-end of the ϕCh1 genome, respectively (Klein et al., 2002). Deletion of ORF59 leads to undetectable levels of PCNA, Mtase, gp34, and protein E in *N. magadii* L11-ΔPCNA (pNB102) when analysed via Western blot (Fig. 4, panel 2). Complementation with each of the ORF59 variants results in a return to detectable levels of all proteins (Fig. 4, panels 3, 4, and 5). However, the protein production kinetics differ between complemented strains and these differences vary between the proteins analysed.

The blots with α-PCNA_2 (Fig. 4A) indicate that *N. magadii* L11-ΔPCNA (pPCNA-GTG) has a similar protein production kinetic to *N. magadii* L11 (pNB102) although a lower level of protein. The ATG exchange strain *N. magadii* L11-ΔPCNA (pPCNA-ATG) has a higher production of PCNA than any of the other analysed strains at all analysed time points (Fig. A5 A). The truncated ORF59 expressing strain has similar levels of PCNA protein to the GTG expressing ORF59 strain for the first five time points but decreases considerably compared to all other strains at 144 and 168 h.

Western blots using α-E do not reveal significant differences in major capsid protein E production kinetics between the complemented strains. The *N. magadii* L11-ΔPCNA (pPCNA-GTG) expression strain produces slightly more protein than either the ATG exchanged or truncated strains. The blots also reveal that none of the strains produces as much capsid protein as *N. magadii* L11 (pNB102), possibly an indication as to why the virus titer levels in the complemented deletion strains are not as high as the wild type.

α-gp34 blots show a higher amount of protein in the GTG and ATG exchanged ORF59 expressing strains than *N. magadii* L11 (pNB102) (Fig. 4C). The ATG exchanged ORF59 expressing strain has detectable levels of gp34 in each of the time points, in contrast to the wild type control which has no detectable levels in the first two and final time points. The GTG expressing strain has detectable gp34 levels 24, 48 and 168 h after inoculation when it is not detectable in the wild-type strain. The truncated ORF59 expressing strain has the lowest levels of detectable protein of the complemented strains with a small amount detectable at 24 h, likely remaining from the previous passage and otherwise detectable protein in only the 72 and 96-hour time

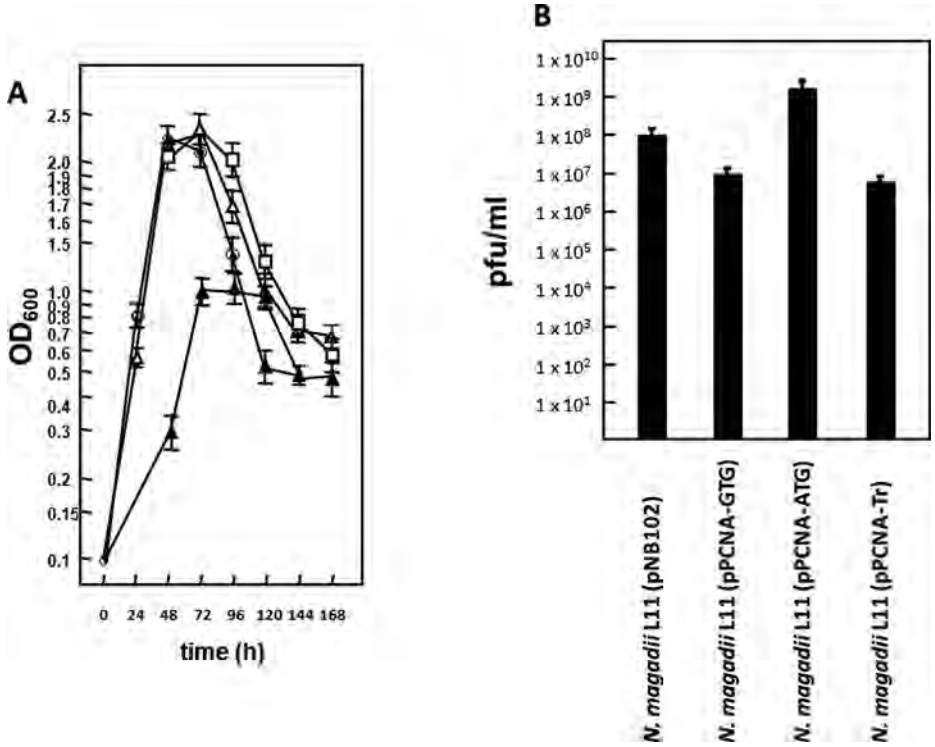


**Fig. 5.** Growth and virus progeny production of the overexpressing strains (A) Growth curves of the overexpressing strains: *N. magadii* L11 (pPCNA-GTG) (△), *N. magadii* L11 (pPCNA-ATG) (▲) and *N. magadii* L11 (pPCNA-Tr) (❒) with *N. magadii* L11 (pNB102)) (●) included as a control. (B) Virus titers of the overexpressing strains at 96 h with *N. magadii* L11 (pNB102) included as a control. Error bars are indicated, ±1SD. 3 technical replicates were used.

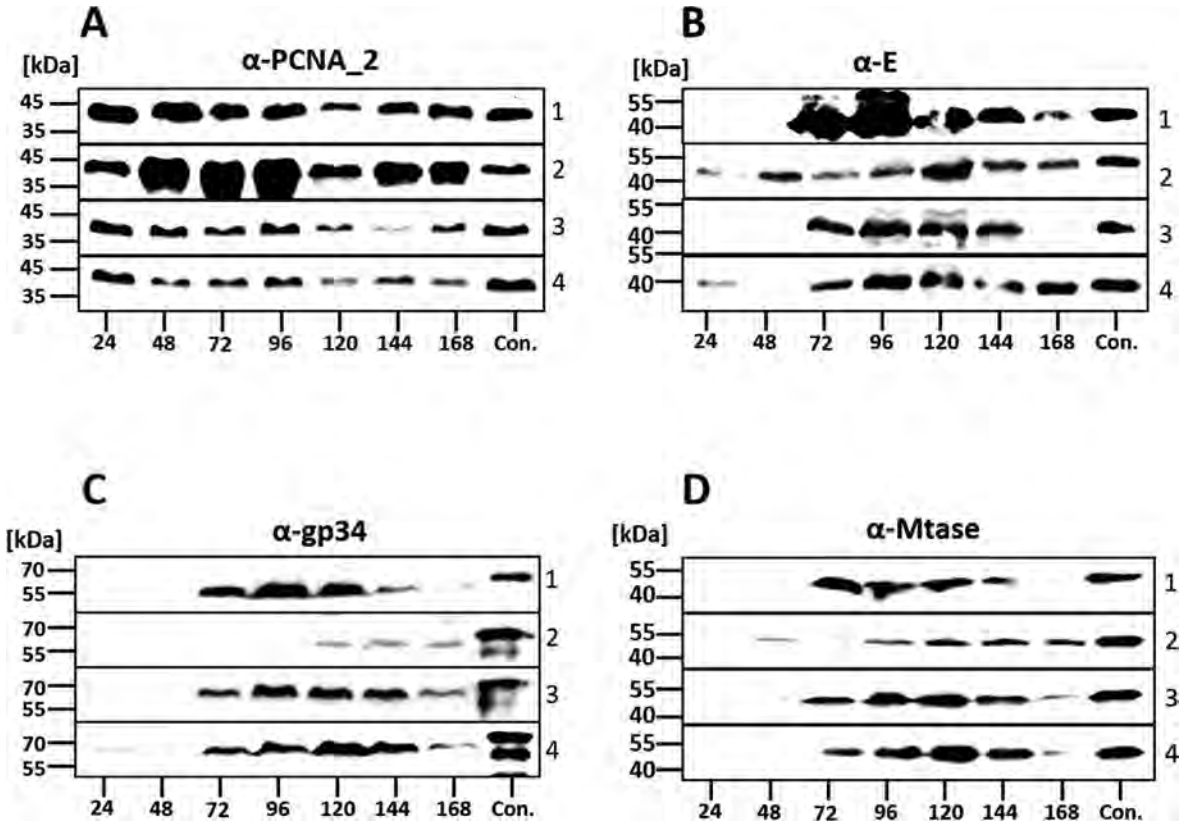


**Fig. 6.** Protein levels of the over expressing strains as measured by Western blot. (A) α-PCNA-2 (B) α-E (C) α-gp34 (D) α-Mtase. 1) *N. magadii* L11 (pNB102), 2) *N. magadii* L11 (pPCNA-ATG), 3) *N. magadii* L11 (pPCNA-Tr), 4) *N. magadii* L11 (pPCNA-GTG). Lanes 1 to 7: samples were taken 24 to 168 h after inoculation. Con: proteins isolated from *E. coli* were taken as a control (lane 8 in each panel). Size markers are indicated at the left. 3 technical replicates were used.

point samples. This indicates that the 21-amino acid N-terminal extension of $PCNA_{\Phi Ch}$ helps to regulate the production of gp34.

Western blots with α-Mtase show an earlier production of Mtase in the ATG exchanged ORF59 complemented strains, lower levels and extended production in the truncated ORF59 expressing strain, and very high protein levels at 96 and 120 h in the GTG variant expressing strain. Again, this demonstrates the differential regulation of proteins by the variants of ORF59. Densitometry analysis of all overexpression Western blots are given in Fig. 5A.

### 3.4. Analysis of overexpressing strains

#### 3.4.1. Growth curves and virus titers of overexpressing strains

The presence of pPCNA-ATG leads to a significant reduction of the growth of *N. magadii* L11 during the exponential phase (Fig. 5A). *N. magadii* L11 (pPCNA-GTG) and *N. magadii* L11 (pPCNA-Tr) have a similar growth rate in the exponential phase and a similar rate of lysis after a slightly delayed onset in comparison to *N. magadii* L11 (pNB102). The strains transformed with the pPCNA-GTG and pPCNA-Tr plasmids showed a slight reduction in virus particle production compared to both *N. magadii* L11 (pNB102) and *N. magadii* L11 at 168 h (Fig. 5B).

The virus titer of *N. magadii* L11 (pPCNA-ATG) has an altered kinetic of virus particle production. Compared to *N. magadii* L11 (pNB102) it produces at least one magnitude more virus particles for the first four days of the time series and an equal amount on day five (Fig. A4). *N. magadii* L11 (pPCNA-GTG) and *N. magadii* L11 (pPCNA-Tr) have virus progeny counts higher than the control strain on days one and two, while *N. magadii* L11 (pNB102) has higher virus titers on the final four time points (Fig. A4).

*N. magadii* L11 (pPCNA-ATG) has a significantly altered growth and lysis phenotype. This strain has a retarded growth profile during the exponential growth phase and has a significantly lower optical density than all other strains until the late lytic phase (Fig. 5A).

#### 3.4.2. Protein production of overexpressing strains

Western blots using α-PCNA_2 (Fig. 6A). revealed that *N. magadii* L11 (pPCNA-ATG) had an exceptionally high amount of detectable $PCNA_{\phi Ch1}$ in comparison to any of the other strains. Indicating that a mutation of GTG > ATG at the 5′ end of the extension of ϕCh1 ORF59 results in a strong over production of $PCNA_{\Phi Ch1}$. The levels of protein in *N. magadii* L11 (pPCNA-GTG) and *N. magadii* L11 (pPCNA-Tr) are lower than in the wild type control *N. magadii* L11 (pNB102), in agreement with the virus titer levels.

Western blots with α-E (Fig. 6B) show, as in the complemented deletion strains, considerable variation between the strains. *N. magadii* L11 (pPCNA-ATG) has detectable levels of protein E at all seven time points, *N. magadii* L11 (pPCNA-Tr) only has detectable protein E levels from 72 to 144 h, while *N. magadii* L11 (pPCNA-GTG) protein E is only detectable from 72hrs onwards, the visible band at 24hrs is believed to be carry-over from the preculture used for inoculation.

gp34 levels (Fig. 6C) in *N. magadii* L11 (pNB102) peak earlier and at a higher intensity than in either *N. magadii* L11 (pPCNA-GTG) or *N. magadii* L11 (pPCNA-Tr) which both have very similar kinetics and protein levels. However, the levels in *N. magadii* L11 (pPCNA-ATG) are reduced in comparison to *N. magadii* L11 (pNB102) and the other overexpression strains. This may not be due to a reduced production of gp34, but rather the increased rate of early lysis, which reduces the build-up of the protein in the host cells and instead may increase the amount of protein in the supernatant.

As with the protein levels of $PCNA_{\Phi ch1}$, protein E and gp34, the levels of Mtase (Fig. 6D) are broadly similar in *N. magadii* L11 (pNB102), *N. magadii* L11, *N. magadii* (pPCNA-GTG) and *N. magadii* L11 (pPCNA-Tr), they do however peak in concentration 24–48 h later in the two overexpression strains and Mtase is detectable in both at 168 h which it is not in the control strain. As with the three other analysed proteins, the *N. magadii* L11 (pPCNA-ATG) western blot with α-Mtase reveals significant differences to the wild-type control and the other overexpression strains. Mtase is detectable 24 h earlier than in the other strains and is otherwise present at much lower levels in the other time point samples. The lower levels may again be due to the high rate of lysis reducing the build-up of viral proteins in the host

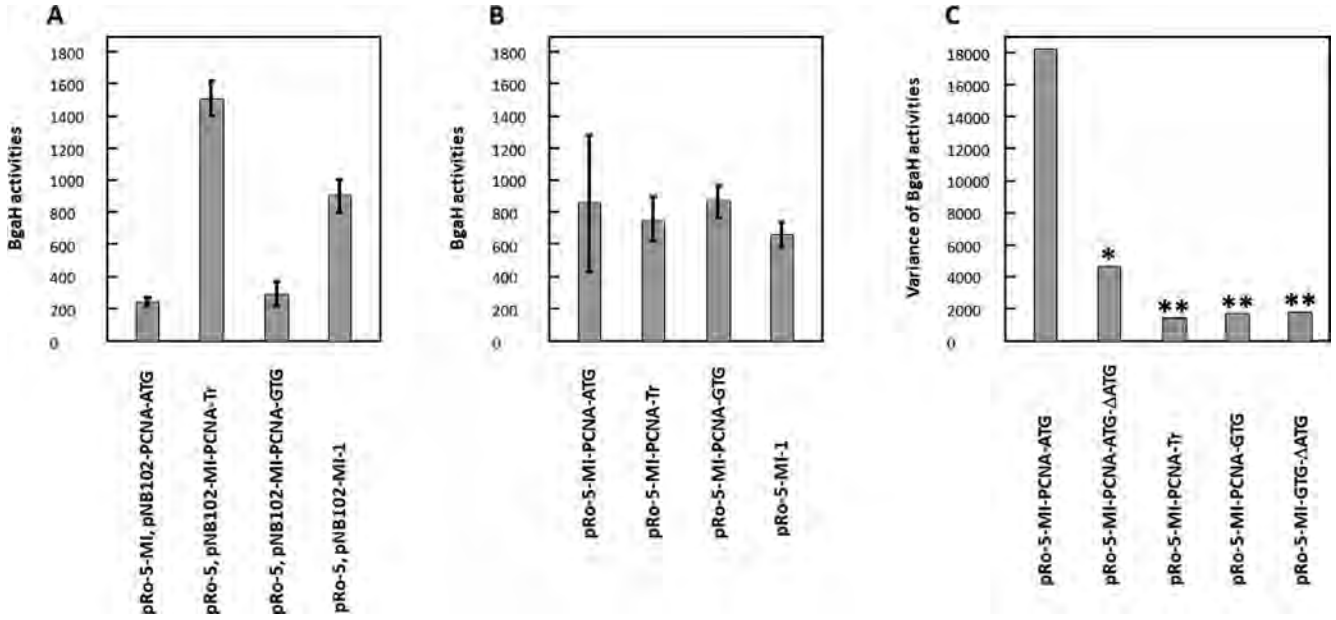


**Fig. 7.** BgaH activities of transformed *N. magadii* L13 strains. (A) Specific BgaH activities taken 108 h after inoculation of *N. magadii* L13 strains transformed with both the pMI-1 plasmid containing the *bga*H reporter gene and a plasmid containing one of the ORF59 variants. (B) Specific BgaH activities taken 108 h after inoculation of *N. magadii* L13 strains transformed with a pMI-1 plasmid containing both the *bga*H reporter gene and one of the ORF59 variants. (C) Variance in BgaH activity of *N. magadii* L13 transformed with plasmids containing both the *bga*H gene and one of the variants of ORF59 measured 48 h after entry into the stationary phase. For all experiments, 5 biological replicates were used. Error bars are indicated, ±1SD. Statistically significant differences in variance between pRo-5-pMI-PCNA-ATG and all other strains was determined by F test and is indicated (* $P \leq 0.05$, ** $P \leq 0.01$).

cells. Densitometry analysis of all overexpression Western blots are given in Fig. 6A.

### 3.5. Interaction of ORF59 and the ϕCh1 origin of replication

To investigate a possible interaction between ORF59 and the ϕCh1 origin of replication, *N. magadii* L13 cells were co-transformed with two plasmids: one containing a variant of ORF59, the other encoding both the origin of replication of ϕCh1 and a *bga*H gene, encoding a halophilic protein with ß-galactosidase activity ((Holmes and Dyall-Smith, 2000). If there is an interaction between ORF59 and the ϕCh1 origin of replication an increase or decrease in the copy number of the plasmid containing the ϕCh1 origin of replication and the *bga*H gene could be determined by a change in the measured BgaH activity due to the gene dosage effect. It was expected that the ORF59 variants potentially encoding for the larger $PCNA_{\Phi Ch1}$ would result in an increased replication of plasmids containing the ϕCh1 origin of replication and therefore a higher measured BgaH activity.

The highest BgaH activity was observed for *N. magadii* L13 (pRo-5/pPCNA-Tr) (Fig. 7A). This strain also obtained a much higher peak optical density compared to the other three strains (data not shown). Lower BgaH activities compared to the control were observed for the *N. magadii* L13 (pRo-5/pPCNA-ATG) and *N. magadii* L13 (pRo-54/pPCNA-GTG) strains, possibly indicating an inhibition of plasmid replication by the two longer variants of ORF59.

The results of the double plasmid transformant experiment did not behave as expected. This in combination with the partial rescue of viral phenotypes (Figs. 3 and 4) led to the hypothesis that there may be differential effects when ORF59 is encoded *in cis* or *in trans*. To investigate this possibility further an additional experiment was designed wherein *N. magadii* L13 was transformed with a single plasmid containing both the origin of replication of ϕCh1 and a version of ORF59 encoded on a single plasmid in addition to the *bga*H reporter gene.

The results from the single plasmid experiment showed strong variations in phenotype compared to the results obtained from the double plasmid experiments (Fig. 7B). This data seems to demonstrate that the different gene variants have different effects when they are expressed in *cis* or *trans* relative to the origin of replication of ϕCh1. However, these results are compounded upon a closer examination of the individual biological replicates of *N. magadii* L13 (pMI-PCNA-ATG) where there is a large variance in the BgaH activities measured between individual clones($n = 3$). To determine if this was an artifact or an inherent behaviour of the variants a new experiment was designed.

In this experiment the pMI-PCNA plasmids were retransformed into *N. magadii* L13 in addition to two new plasmids. The additional plasmids were constructed as variants of the ATG and GTG variants where a point mutation was introduced to remove the AUG start codon homologous to the *N. magadii* PCNA start codon, such that translation could only start from the GUG or AUG start codons resulting in the longer ϕCh1 PCNA variant. Therefore, the AUG codons were changed to CUG. For each of the transformed strains a minimum of 5 clones were analysed.

The data indicated that there is a large variance in the BgaH activities measured for the pRo-5-pMI-PCNA-ATG clones and the other strains. The data also indicated that the removal of the second AUG start codon resulted in a set of clones with no statistically significant difference of variance of BgaH activities when measured compared to the other strains. There was also no statistically significant difference in mean between the five different ORF59 variants (data not shown).

## 4. Discussion

Here we report the first experiments concerning the virus encoded PCNA homolog of virus ϕCh1. Upon investigation of the first published sequence of ϕCh1 it was noted that the virus encoded a PCNA homolog, at the time this was noted as unusual for an archaeal virus (Klein et al., 2002). Initial investigations with an antibody developed against the gene product of ORF59 indicated the presence of two bands within a Western blot of a ϕCh1 infected *N. magadii* strain (Fig. 1). Closer examination of the published genome sequence of ϕCh1 revealed the presence of a potential alternate start codon upstream of the canonical AUG start codon. Further experiments were designed to investigate the function of ORF59 and the region thought to be encoded between the GUG and AUG start codons.

Deletion of ORF59 resulted in a significant reduction in the virus titer, viral protein levels, and aberrant lytic behaviour. Three complementation variants resulted in reversal of the lytic phenotype, a variety of effects on the viral protein levels, and a failure to return virus titer levels comparable to the wild type. Overexpression with a full-length wild-type variant and a 5′ truncation variant of ORF59 resulted in a reduction in the virus titer. Contrastingly, overexpression with the ATG point mutation variant of ORF59 induced a significantly increased virus titer in the exponential growth phase and a significantly reduced growth rate.

The analysis of growth and lysis behaviour reveals that ORF59 plays a critical role in the lytic behaviour of ϕCh1, and, that this behaviour is largely regulated by the region downstream of the ATG consensus sequence when compared to the host encoded PCNA. The results of the virus titer and western blot experiments demonstrate that the production of viral progeny is highly sensitive to the amount and variant of ORF59.

The Western blot data provides evidence that the PCNA of ϕCh1 may have additional roles in gene expression and consequently protein production. This possibly indicates that the 21-amino acid N-terminal extension has a significant direct or indirect effect on the proteome of ϕCh1. This could be caused by a number of different factors, including changes in the viral genome copy number resulting in changes to transcriptional regulator levels, lytic repressors and activators, or epigenetic gene expression modulation through interactions of PCNA with epigenetic factors (Pan et al, 2011).

The data provided may indicate that the alternate start codon GUG regulates production of a longer variant of $PCNA_{\Phi Ch1}$. A single point mutation of GTG to ATG results in a significant increase in early virus titer, proteins detectable with α-PCNA_2 Western blots, and a significant reduction in the growth kinetics, when expressed from a plasmid in the wild-type strain. Intriguingly, when the ATG variant is expressed in the ORF59 mutant background it does not significantly differ in behaviour from the strains expressing the GTG and truncated variants of ORF59.

The data indicates that the stoichiometric balance of the inferred long and short variants of $PCNA_{\Phi Ch1}$ and potentially the PCNA of *N. magadii* is important for a well-regulated life cycle of virus ϕCh1. However, this would require an in-depth transcriptomic and proteomic analysis of the interactions between the different variants of PCNA within ϕCh1 infected *N. magadii* cells.

The experiments investigating potential interactions between $PCNA_{\phi Ch1}$ and the origin of replication of ϕCh1 indicated that there are interactions between the two. These interactions appear to be modulated by the N-terminal region encoded by the GTG to ATG sequence of ORF59. These experiments indicated a potential inhibitory activity of the longer $PCNA_{\phi Ch1}$ when encoded *in trans* and an activating activ-

## Appendix A

*Plasmids used in this study*

| Name | Description | |
|---|---|---|
| pRSET-A | mcs, *bla*, ColE1, His-tag | Invitrogen |
| pPol5 | ORF59 in pRSET-A | *This study* |
| pKSII + | Cloning vector for *E. coli* | Stratagene |
| pUC19 | Cloning vector for *E. coli* | Celeste et al., 1985 |
| pUC19-NovR "reverse" | *gyr*B gene in pUC19 in the reverse orientation | *This study* |
| pKSII-PCNA1-5-NovR-R | Suicide plasmid for the disruption of ORF59 with *gyr*B (*bla*) | *This study* |
| pKS-34up | Promotor of ORF34 in PKSII + | *This study* |
| pKS-34up-PCNA-ATG | ΦCh1-ORF59 with a point mutation of GTG > ATG under the control of the promoter of ΦCh1-ORF34 in pKSII + | *This study* |
| pKS-34up-PCNA-Tr | 5′ truncated ΦCh1-ORF59 under the control of the promoter of ΦCh1-ORF34 in pKSII + | *This study* |
| pKS-34up-PCNA-GTG | ϕCh1-ORF59 under the control of the promoter of ϕCh1-ORF34 in pKSII + | *This study* |
| pNB102 | Shuttle vector (*bla*, *Mev*$^{R}$) | Zhou et al, 2004 |
| pPCNA-ATG | ϕCh1-ORF59 with a point mutation of GTG > ATG under the control of the promoter of ϕCh1-ORF34 in pNB102 | *This study* |
| pPCNA-GTG | ϕCh1-ORF59 under the control of the promoter of ϕCh1-ORF34 in pNB102 | *This study* |
| pPCNA-Tr | 5′ truncated ϕCh1-ORF59 under the control of the promoter of ORF34 in pNB102 | *This study* |
| pRo-5/BgaH | bla, ColE1, NovR, ϕCh1 ori, intergenic region, bgaH | Mayrhofer-Iro et al., 2013 |
| pMI-PCNA-ATG | pRo-5/BgaH, ϕCh1-ORF59 with a point mutation of GTG > ATG under the control of the promoter of ϕCh1-ORF34 | *This study* |
| pMI-PCNA-TR | pRo-5/BgaH, 5′ truncated ϕCh1-ORF59 under the control of the promoter of ORF34 | *This study* |
| pMI-PCNA-GTG | pRo-5/BgaH, ΦCh1-ORF59 under the control of the promoter of ϕCh1-ORF34 | *This study* |
| pMI-PCNA-ATG-ΔATG | pRo-5/BgaH, ΦCh1-ORF59 with a point mutation of ATG > CTG under the control of the promoter of ϕCh1-ORF34 | *This study* |
| pMI-PCNA-GTG-ΔATG | pRo-5/BgaH, ϕCh1-ORF59 with a point mutation of ATG > CTG under the control of the promoter of ϕCh1-ORF34 | *This study* |

*Strains used in this study*

| Name | Description | Reference |
|---|---|---|
| *N. magadii* L13 | cured strain | Witte et al, 1997 |
| *N. magadii* L11 | wild-type strain, ϕ Ch1 provirus | Witte et al., 1997 |
| *N. magadii* L11-ΔPCNA | deletion of ϕCh1-ORF59 by *gyr*B | *This study* |
| *E. coli* BL21(DE3) | *E. coli* str. B F$^{-}$ *ompT gal dcm lon hsdS*$_B$($r_B^- m_B^-$) λ(DE3 [*lacI lacUV5-T7p07 ind1 sam7 nin5*]) [*malB*$^+$]$_{K\text{-}12}$($\lambda^S$) | Novagen |
| *E. coli* XL1-Blue | *end*A1 *gyr*A96(nal$^R$) thi-1 *rec*A1 *rel*A1 *lac gln*V44 F'[::*Tn*10 proAB$^+$ *lac*I$^q$ Δ(*lac*Z)M15 Amy Cm$^R$] *hsd*R17($r_K^+$ $m_K^+$) | Stratagene |

*Primers used in this study*

| Primer name | Primer Sequence (5′-3′) |
|---|---|
| p30-5 | CAGCAGAGATCTATGTTCAAAGCAATCGCTAC |
| p30-3 | CAGCAGAAGCTTTCAGTTGCTCTGGATCCG |
| ΔPCNA-1 | GATCTCTAGAGAAGTGCTACCGCTGCA |
| ΔPCNA-2 | GAATCCCGGGAGCTCAGCGTGCTCGA |
| ΔPCNA-3 | GTATAAGCTTCCAGAGCAACTGAGTGATCA |
| ΔPCNA-5 | GATCGGTACCGTCCCGCATGCACTCAG |
| NovR-1p | GATCCTGCAGTGTCGACTGGAACGAGG |
| NovR-1s | GATCCCCGGGTGTCGACTGGAACGAGG |
| 56–5 | CAGCAGGATCCATGAGAGAGAACAATCC |
| Nov-13 | GACGCCGAATGGGTAGAC |
| Nov-12 | GCCGGTGAGTACTTAACGC |
| PCNA-3en | GTCGACGATCTCCGCTAGCT |
| 34-p5-XbaI | CAG CAG TCT AGA ATC GGG TGG GAT CCC |
| 34-p3 | GACGACGGATCCTGTGTTACCTCGTAGCTCTGG |
| PCNA-ATG | GTTCGAATTCATGCGGTATCGACCAGGACC |
| PCNA-22 | GACAGGTACCTCAGTTGCTCTGGATCCGC |
| PCNA-Tr | GTTCGAATTCATGTTCAAAGCAATCGCTACGA |
| PCNA-GTG | GTTCGAATTCGTGCGGTATCGACCAGGACC |
| IR-PCNA-1_1 | GAATTGGAGCTCCACCGCGGTGGCATCGGGTGGGATCCCGACGCGATTT |
| IR-PCNA-2_1 | AGAAGCTGCCTTCAACGCGGCGGCCTCAGTTGCTCTGGATCCGCGGCGAG |
| PCNA-ΔATG-2 | CTTCGTAGCGATTGCTTTGAACAGTGGTGTGGTTTCTGATTGGTTCAGGCTC |
| PCNA-ΔATG-1 | GAGCCTGAACCAATCAGAAACCACACCACTGTTCAAAGCAATCGCTACGAAG |

ity when encoded *in cis,* whereas the truncated gene has a strong activating effect when encoded *in cis*. Intriguingly the BgaH activities of the ATG mutant ORF59, when encoded *in trans,* has a high variability between individual clones. This variability is significantly reduced by the removal of the canonical AUG start codon. For both possible start codons there is the potential for the use of different ribosome binding sites (Klein et al 2002). The removal of the second AUG start codon would result in only a single protein, altering the stoichiometry, again indicating the potential importance of the stoichiometric balance of PCNA variants on the ϕCh1 life cycle. The results of these experiments go some way to explaining the partial rescue of the phenotypes in the complemented strains and the differential effects in the overexpression strains.

## 5. Conclusion

The viral encoded $PCNA_{\phi Ch1}$ is not essential but is crucial to the life cycle of the virus ϕCh1. The sequence encoded between the alternate GUG and canonical AUG start codons is not essential to the function of the viral homolog. However it does modify the phenotypic behaviour of strains when expressed from a plasmid in both complementation and overexpression contexts, particularly when the GUG start codon is mutated to an AUG.

One function of the viral protein seems to be to direct the replication machinery of *N. magadii* towards replication of viral DNA instead of replication of host chromosomal DNA. This is supported by the BgaH assay experiments demonstrating differential *in cis* and *in trans* influences of the ORF59 variants on plasmid replication.

The modifications of the viral PCNA compared to the host PCNA demonstrate the potential for modulation of gene expression by PCNA mediated by alternate start codon usage and an N-terminal extension, directly or indirectly.

## Declaration of Competing Interest

The authors declare that they have no known competing financial interests or personal relationships that could have appeared to influence the work reported in this paper.

## Acknowledgments

Dina Ada Sabic for assisting with the Western blot analysis and Kristina Vasilijevic for her assistance with the BgaH experiments

## Appendix B. Supplementary data

Supplementary data to this article can be found online at https://doi.org/10.1016/j.crbiot.2022.09.006.

## References

Acharya, S., Dahal, A., Bhattarai, H.K., Lustig, A.J., 2021. Evolution and origin of sliding clamp in bacteria, archaea and eukarya. PLoS ONE 16 (8), e0241093. https://doi.org/10.1371/journal.pone.0241093.

Babski, J., Haas, K.A., Näther-Schindler, D., Pfeiffer, F., Förstner, K.U., Hammelmann, M., Hilker, R., Becker, A., Sharma, C.M., Marchfelder, A., Soppa, J., 2016. Genome-wide identification of transcriptional start sites in the haloarchaeon Haloferax volcanii based on differential RNA-Seq (dRNA-Seq). BMC Genomics 17 (1), 1–19. https://doi.org/10.1371/journal.pone.0215986.

Baranyi, U., Klein, R., Lubitz, W., Krüger, D.H., Witte, A., 2000. The archaeal halophilic virus-encoded Dam-like methyltransferase M.ϕCh1-I methylates adenine residues and complements *dam* mutants in the low salt environme39nt of *Escherichia coli*. Mol. Microbiol. 35 (5), 1168–1179. https://doi.org/10.1046/j.1365-2958.2000.01786.

Celeste, Y.P., Vieira, J., Messing, J., 1985. Improved M13 phage cloning vectors and host strains: nucleotide sequence of the M13mpl8 and pUC19 vector. Gene 33 (1), 103–119. https://doi.org/10.1016/0378-1119(85)90120-9.

Dionne, I., Nookala, R.K., Jackson, S.P., Doherty, A.J., Bell, S.D., 2003. A heterotrimeric PCNA in the hyperthermophilic archaeon Sulfolobus solfataricus. Mol. Cell 11 (1), 275–282. https://doi.org/10.1016/S1097-2765(02)00824-9.

Dyall-Smith, M., 2009. The halohandbook: protocols for halobacterial genetics, version 7.2. Available from: <https://haloarchaea.com/halohandbook/>.

Gibson, D.G., Young, L., Chuang, R.-Y., Venter, J.C., Hutchison, C.A., Smith, H.O., 2009. Enzymatic assembly of DNA molecules up to several hundred kilobases. Nat. Methods 6 (5), 343–345. https://doi.org/10.1038/nmeth.1318.

Gropp, F., Grampp, B., Stolt, P., Palm, P., Zillig, W., 1992. The immunity-conferring plasmid pφHL from the Halobacterium salinarium phage φH: nucleotide sequence and transcription. Virology 190 (1), 45–54. https://doi.org/10.1016/0042-6822(92)91191-V.

Harlow, E.D., Lane, D., 1988. A Laboratory Manual. Cold Spring Harbor Laboratory, New York, p. 579.

Holmes, M.L., Dyall-Smith, M.L., 2000. Sequence and expression of a halobacterial b-galactosidase gene. Mol. Microbiol. 36 (1), 114–122. https://doi.org/10.1046/j.1365-2958.2000.01832.x.

Holmes, M.L., Nuttall, S.D., Dyall-Smith, M.L., 1991. Construction and use of halobacterial shuttle vectors and further studies on Haloferax DNA gyrase. J. Bacteriol. 173 (12), 3807–3813. https://doi.org/10.1128/jb.173.12.3807-3813.1991.

Iro, M., Klein, R., Galos, B., Baranyi, U., Rossler, N., Witte, A., 2007. The lysogenic region of virus ϕCh1: identification of a repressor-operator system and determination of its activity in halophilic *Archaea*. Extremophiles 11 (2), 383–396. https://doi.org/10.1007/s00792-006-0040-3.

Kazlauskas, D., Krupovic, M., Venclovas, Č., 2016. The logic of DNA replication in double-stranded DNA viruses: insights from global analysis of viral genomes. Nucleic Acids Res. 44 (10), 4551–4564. https://doi.org/10.1093/nar/gkw322.

Klein, R., Greineder, B., Baranyi, U., Witte, A., 2000. The structural protein E of the archaeal virus ϕCh1: evidence for processing in Natrialba magadii during virus maturation. Virology 276 (2), 376–387. https://doi.org/10.1006/viro.2000.0565.

Klein, R., Baranyi, U., Rössler, N., Greineder, B., Scholz, H., Witte, A., 2002. Natrialba magadii virus ϕCh1: first complete nucleotide sequence and functional organization of a virus infecting a haloalkaliphilic archaeon. Mol. Microbiol. 45 (3), 851–863. https://doi.org/10.1046/j.1365-2958.2002.03064.x.

Klein, R., Rössler, N., Iro, M., Scholz, H., Witte, A., 2012. Haloarchaeal myovirus ϕCh1 harbours a phase variation system for the production of protein variants with distinct cell surface adhesion specificities. Mol. Microbiol. 83 (1), 137–150. https://doi.org/10.1111/j.1365-2958.2011.07921.

Ladner, J.E., Pan, M., Hurwitz, J., Kelman, Z., 2011. Crystal structures of two active proliferating cell nuclear antigens (PCNAs) encoded by Thermococcus kodakaraensis. Proc. Natl. Acad. Sci. 108 (7), 2711–2716. https://doi.org/10.1073/pnas.1019179108.

Lynch, E.A., Langille, M.G., Darling, A., Wilbanks, E.G., Haltiner, C., Shao, K.S., Starr, M. O., Teiling, C., Harkins, T.T., Edwards, R.A. and Eisen, J.A., 2012. Sequencing of seven haloarchaeal genomes reveals patterns of genomic flux. doi: 10.1371/journal.pone.0041389

Maga, G., Hubscher, U., 2003. Proliferating cell nuclear antigen (PCNA): a dancer with many partners. J. Cell Sci. 116 (15), 3051–3060. https://doi.org/10.1242/jcs.00653.

Mayrhofer-Iro, M., Ladurner, A., Meissner, C., Derntl, C., Reiter, M., Haider, F., Dimmel, K., Rössler, N., Klein, R., Baranyi, U., Scholz, H., Witte, A., 2013. Utilization of virus ϕCh1 elements to establish a shuttle vector system for halo(alkali)philic archaea via transformation of Natrialba magadii. Appl. Environ. Microbiol. 79 (8), 2741–2748. https://doi.org/10.1128/AEM.03287-12.

Mizuno, C.M., Prajapati, B., Lucas-Staat, S., Sime-Ngando, T., Forterre, P., Bamford, D. H., Prangishvili, D., Krupovic, M., Oksanen, H.M., 2019. Novel haloarchaeal viruses from Lake Retba infecting Haloferax and Halorubrum species. Environ. Microbiol. 21 (6), 2129–2147. https://doi.org/10.1111/1462-2920.14604.

Moldovan, G.L., Pfander, B., Jentsch, S., 2007. PCNA, the maestro of the replication fork. Cell 129 (4), 665–679. https://doi.org/10.1016/j.cell.2007.05.003.

Pan, M., Kelman, L.M., Kelman, Z., 2011. The archaeal PCNA proteins. Biochem. Soc. Trans. 39 (1), 20–24. https://doi.org/10.1042/bst0390020.

Rössler, N., Klein, R., Scholz, H., Witte, A., 2004. Inversion within the haloalkaliphilic virus ϕCh1 results in differential expression of structural proteins. Mol. Microbiol. 52 (2), 413–426. https://doi.org/10.1111/j.1365-2958.2003.03983.x.

Selb, R., Derntl, C., Klein, R., Alte, B., Hofbauer, C., Kaufmann, M., Beraha, J., Schöner, L., Witte, A., 2017. The viral gene ORF79 encodes a repressor regulating induction of the lytic life cycle in the haloalkaliphilic virus ϕCh1. J. Virol. 91 (9), e00206–e217. https://doi.org/10.1128/JVI.00206-17.

Stoimenov, I., Helleday, T., 2009. PCNA on the crossroad of cancer. Biochem. Soc. Trans. 37 (3), 605–613. https://doi.org/10.1042/BST0370605.

Tindall, B.J., Mills, A.A., Grant, W.D., 1984. *Natronobacterium* gen nov. and *Natronococcus* gen. nov. two genera of haloalkaliphilic archaebacteria. Syst. Appl. Microbiol. 5 (1), 41–57. https://doi.org/10.1016/S0723-2020(84)80050-8.

Winter, J.A., Christofi, P., Morroll, S., Bunting, K.A., 2009. The crystal structure of Haloferax volcanii proliferating cell nuclear antigen reveals unique surface charge characteristics due to halophilic adaptation. BMC Struct. Biol. 9 (1), 1–15. https://doi.org/10.1186/1472-6807-9-55.

Witte, A., Baranyi, U., Klein, R., Sulzner, M., Luo, C., Wanner, G., Krüger, D.H., Lubitz, W., 1997. Characterization of Natronobacterium magadii phage ϕCh1, a unique archaeal phage containing DNA and RNA. Mol. Microbiol. 23 (3), 603–616. https://doi.org/10.1046/j.1365-2958.1997.d01-1879.x.

Zhou, M., Xiang, H., Sun, C., Tan, H., 2004. Construction of a novel shuttle vector based on an RCR-plasmid from a haloalkaliphilic archaeon and transformation into other haloarchaea. Biotechnol. Lett. 26 (14), 1107–1113. https://doi.org/10.1023/b:bile.0000035493.21986.20.